Chemistry, Physics and Technology of Surface. 2024. V. 15. N 4. P. 514-523

UDC 577.1:615.28 + 616-006 + 544.77 doi: 10.15407/hftp15.04.514

Yu.M. Samchenko [1], O.A. Samoylenko [2], A.V. Verbinenko [2], I.I. Ganusevich [2], L.O. Kernosenko [1], T.P. Poltoratska [1], N.O. Pasmurtseva [1], O.O. Solovieva [1], I.I. Volobayev [1]

SYNTHESIS AND APPLICATION OF POLYACRYLAMIDE HYDROGELS WITH INCORPORATED ACID-ACTIVATED LAPONITE® FOR DIAGNOSIS OF ONCOLOGICAL DISEASES

[1] F.D. Ovcharenko Biocolloidal Chemistry Institute of National Academy of Sciences of Ukraine
42 Academician Vernadskogo Blvd., Kyiv 03142, Ukraine, E-mail: yu1sam@yahoo.com
[2] R.E. Kavetsky Institute of Experimental Pathology, Oncology and Radiobiology of National Academy of Sciences of Ukraine
45 Vasylkivska Str., Kyiv, 03022, Ukraine, E-mail: a-samoilenko@ukr.net

Hydrogels with incorporated acid-activated Laponite® (LapA) platelets represent a new generation of biomaterials with promising biomedical application (e.g., diagnostics and therapy). The LapA nanomaterial have high specific surface area and demonstrate rather attractive hydrophilic properties. The physical cross-linking of hydrogels using the LapA allowed a significant improvement the systems homogeneity, transparency, and drug transport in these systems. In general incorporation of LapA may also affect the equilibrium degree of swelling at phase-transition from the swollen to the shrunken phase. In this work the effectiveness of using of polyacrylamide hydrogels (PAAG) with incorporated LapA for diagnosis of oncological diseases was studied. The synthesis procedure was performed using ultrasonication of aqueous dispersion of mixtures of monomer, crosslinking agent and initiators. The PAAG+LapA samples were characterized using SEM and PAAG swelling techniques. SEM images evidenced the presence of integration of LapA platelets into the hydrogel structure and formation of the shells of aggregated LapA particles. It can be explained by the formation of more active forms of LapA with stronger internal bonds. Effects of Lap, LapA concentration on the swelling kinetics and the maximal swelling degree were also evaluated. The the maximal equilibrium degree of swelling Q_{max} was reached within the first 5 hours. The concentration of platelets affected the value of Q_{max}, initially it decreased up to the minimum $Q_{max} \approx 7.6$ g/g at $C_{Lap} \approx 0.04$ % and then increased at higher concentrations. For these samples the protein separation spectrum of peripheral blood plasma was studied using the sodium dodecyl-sulfate polyacrylamide gel electrophoresis (SDS-PAGE) technique. Peripheral blood plasma samples obtained from the donors, and colorectal cancer patients without distant metastases and with distant metastases were studied. The better separation of human plasma proteins was observed in hydrogels with incorporated LapA platelets. In future studies it is desirable to test these new SDS-PAGE materials for diagnostics of different forms of cancer diseases.

***Keywords**: Laponite® platelets, acid activation, swelling, SDS-PAGE, diagnostics of cancer diseases*

INTRODUCTION

Nowadays, different applications of aqueous hydrogels cross-linked by Laponite® (Lap)-based nanomaterials have attracted great attention [1, 2]. The high purity gel-forming synthetic Lap platelets have diameter of ≈ 25 nm, thickness of ≈ 0.92 nm, and can be easily dispersed in distilled water (Fig. 1 *a*) [3, 4]. It has a plate-like structure, belongs to the family of silicates, and shows the excellent colloidal properties [5, 6]. Compared to natural clays, Lap demonstrates high optical transparency, high dispersibility in water, and an excellent colloidal stability in suspensions [7]. Colloidal suspensions of the highly anisometric Lap platelets demonstrates many surprising properties, interesting phase states, "house of cards" assembly, unique structural ordering, and phenomenon of dynamical arrest [8, 9]. Moreover, modified Lap-based materials have found interesting practical applications as the components for household items, agricultural, and horticultural products, personal care and cosmetic products (toothpastes, skincare and sunscreen emulsions, cosmetics, shampoos, creams), biomaterials and additives to the multifunctional composites, adsorbents, catalysts, glass, ceramics, enamels, barriers and polymer films, surface coatings, *etc*. [10–20]. Modification of Lap structure allows fine regulation of different properties of Lap platelets, their dispersibility, surface charge, colloidal stability and affinity toward biomolecules. Lap includes different types of

active sites such as the interlayer, surface, edge and inter-particle sites [21].

Note that physical cross-linking of hydrogels by Lap nanoparticles allowed a significant improvement in the homogeneity and transparency of hydrogels, as well as the transport properties in incorporated drug molecules [14]. The medical–biological applications of functional hydrogels based on polyacrylamide hydrogels (PAAG) (Fig. 1 *b*) have also attracted some attention [22–24]. These hydrogels are extensively cross-linked polymeric systems and they include 2.5–15 % polyacrylamide saturated with water. PAAG also called Interfall (produced in Ukraine) was widely used as injectable dermal filler. However, the PAAG-related complications persisting in patients restrict wide application of PAAG injections [25]. PAAG are conventionally prepared by copolymerization of acrylamide, bis-acrylamide, ammonium persulfate (APS) and N,N,N',N'-tetramethylethylenediamine (TEMED) [26, 27]. Polymerization is initiated by APS, TEMED accelerates the rate of formation of free radicals from APS and these in turn catalyze polymerization.

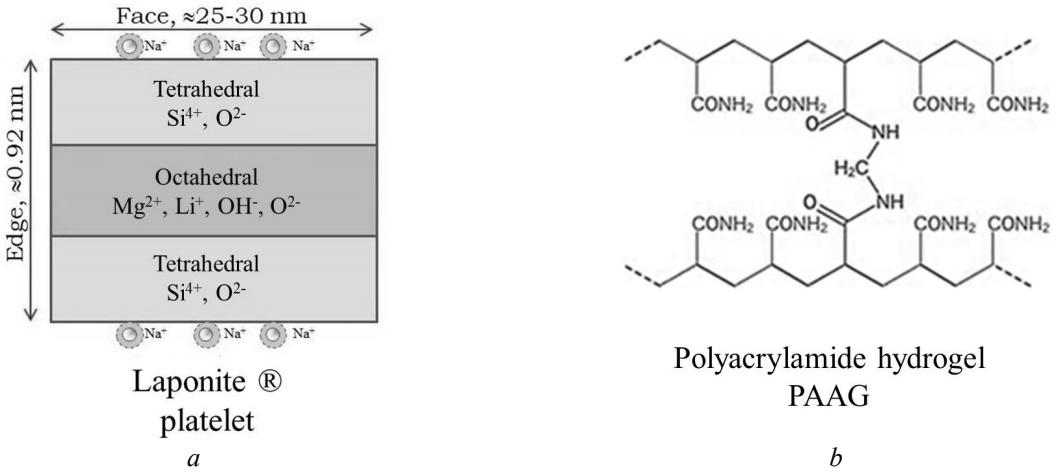

Fig. 1. Schematic presentation of the structures of Laponite® platelets (*a*) and polyacrylamide hydrogel (PAAG) (*b*)

In recent time the materials on the base of polyacrylamide gels began actively used in the early diagnosis of oncological diseases [28]. Different variants of polyacrylamide gel electrophoresis (PAGE) have been developed for identification and quantification of proteins with applications in proteomic analysis [29–32]. The PAGE technique is widely used for fractionalization of proteins in different types of cells (*e.g.*, tumor, blood, or tissue) [29]. The separation of proteins can be improved with gelatin incorporated within the polyacrylamide gel [33] or preparation of PAGE gradient gels [34, 35]. For better quantification in SDS-PAGE technique the strong denaturing sodium dodecyl sulfate detergent (SDS) is used [36, 37].

Incorporation of Lap platelets inside electrophoresis hydrogel systems can affect their efficiency for protein separation. However, to the best of the authors' knowledge, there are no studies on the effects of incorporated of Lap platelets on the quality of proteins separation. This determines the relevance of this study. The present work reports upon experimental studies of effects of incorporated acid-activated Laponite® (LapA) on properties of PAAG hydrogels. The application SDS-PAGE technique for diagnosis of oncological diseases is also discussed.

MATERIALS AND METHODS

Reagents. Acrylamide (AA, C_3H_5NO), "Merck", Darmstadt, Germany), N,N′-methylenebisacrylamide (MBA, $C_7H_{10}N_2O_2$), ammonium persulfate (APS, $(NH_4)_2S_2O_8$), (sodium dodecyl sulphate (SDS, $CH_3(CH_2)_{11}OSO_3Na$), N,N,N',N'-tetramethyl-ethylenediamine (TEMED), tris(hydroxymethyl) aminomethane (TRIS), tetrasodium salt of ethylenediaminetetraacetic acid (Trilon B), high-quality glycerol, diaminodiphenyl sulfone (DDS), bromophenol blue (BPB), sulfuric (H_2SO_4), polyphosphoric (H_3PO_4), hydrochloric (HCl) acids, and Coomassie Brilliant blue G 250

(CI 42655) (all products from Sigma-Aldrich) were used as received without further purification. Double-distilled water was used as a solvent in all experiments.

Pristine Lap and acid-activated Lap (LapA). The gel-forming Laponite ® (Lap) (Fig. 1 *b*) of a personal care grade XLG with empirical formula $Si_8Mg_{5.45}Li_{0.4}H_4O_2Na_{0.7}$ (Rockwood Additives Ltd., Widnes, U.K.) was used in this study. A personal care grade XLG is a purer grade with certified low heavy metal and low microbiological content [1]. In a dry state, the bulk density of Lap powder is 1 g/cm^3, while the particle density is 2.53 g/cm^3 [38].

For preparation of LapA the pristine Lap was dispersed in water using an ultrasonic bath SONOPULS HD 4050 (Bandelin Electronic GmbH). Then an aqueous solution of H_2SO_4 was slowly added, the mixture was stirred for 5 h at room temperature, $T = 25$ °C. The concentration of Lap in the final solution was fixed at 4 wt. %. The preparation of acid activated sample LapA was done in sulphate acid H_2SO_4 dispersions with fixed acid concentration $C_a = 9.1$ % wt. At this C_a the specific surface area of LapA samples was near the maximum, $S \approx 488$ m^2/g [39]. The reaction mixtures were intensively stirred for 2 h at 70 °C, then the LapA samples were washed from unreacted H_2SO_4 acid with distilled water (with repeated replacement) for three days to pH 7.0 and dried at 50 °C.

Preparation of PAAG+Lap and PAAG+LapA hydrogels. Synthesis of the PAAG hydrogels physically cross-linked with Lap or LapA platelets was performed via *in situ* free radical polymerization. The mixtures of Lap or LapA dispersions, AA, MBA was added to the TRIS-buffer solutions (TRIS (10 g), Trilon B (0.25 g) in 175 ml of distilled water and pH 8.9 adjusted using 50 % H_3PO_4 acid). Cross-linking with the spatial network formation occurred due to copolymerization with a bifunctional monomer MBA. The samples were dispersed using a magnetic stirrer (MM-5, 1200 rpm) for 30 min. Then the mixture was additionally dispersed in ultrasonic bath for 30 min, bubbled by argon for 2 min and the redox initiating mixtures (0.75 mL of 0.2 g APS in 4.5 g H_2O and 0.5 g TEMED in 4.5 g H_2O) were added. The resulting mixture was poured between two glass plates separated by 1 mm spacers and kept for 15 min at 25 °C. Preliminary investigations have shown that hydrogels with optimal transparency and physico-mechanical properties can be obtained at 15 % concentration of AA and 0.3 % concentration of cross-linking agent. For more details see [31].

Peripheral blood plasma samples. Donors and patients with colorectal cancer participated in these examinations. These persons underwent a course of treatment in the liver, pancreas and oncovascular surgery department of the National Cancer Institute of the Ministry of Health of Ukraine in 2020–2022. All patients gave written consent to the use of their material for scientific purposes. The study was approved by the Bioethical Committee of the National Academy of Sciences of Ukraine. Peripheral blood plasma of different patients were investigated. The samples were dissolved in 0.4 M TRIS-HCl (pH 6.8) buffer containing glycerol (5 %), DDS (0.1 %) and BPB (0.001 %) mixture.

Determination of the specific surface area of Lap and LapA samples. The specific surface area in the dry state, *S,* was determined using low temperature nitrogen adsorption isotherms recorded at –195.8 °C using a Sorptomatic 1990 apparatus (Thermo Finnigan, USA). Particularly, for Lap samples the specific surface area was $S \approx 307$ m^2/g and the total value of *S* of the completely exfoliated Lap particles was estimated as $S = 930$–970 m^2/g [3]. The acid activation at $C_a = 2$N allowed significant increasing in its specific surface area up to $S \approx 480$ m^2/g (by ≈ 1.56 times) with preservation of hydrophilic properties of LapA samples [39]. Note that this value of *S* was near the maximum. The strong acid activation resulted in significant decreasing of *S*. These changes in *S* reflected the destruction of structure of primary particles and leaching of metal ions from the crystal lattice.

Scanning electron microscopy (SEM). Morphology and porous structure of hydrogel sponges were studied using a Tescan Miga Z LMU scanning electron microscope (SEM) equipped with an Oxford X-Max 80 energy dispersive spectrometer with a PECS Gatan 682 sample preparation system. Sample fragments were attached to an adhesive conductive substrate (carbon tape SPI 05081-AB on the SPI 01506-MB research table). The sample fixed in this way was covered with an ultra-thin (30 nm) layer of conductive material (Au/Pd mixture) using a PECS Gatan 682 device in order to avoid local charge accumulation during SEM analysis.

Swelling of hydrogels. The equilibrium degree of swelling of hydrogels in distilled water, Q, was calculated using the relation

$$Q=(m_s-m_d)/m_d,$$

where m_s is the mass of the swollen hydrogel in the equilibrium state after 24 h of swelling, and m_d is the mass of the completely dried sample after water evaporation.

The hydrogel samples were incubated in a TS-1/80 SPN thermostat and weighed with an accuracy of 10^{-4} g using an AXIS analytical balance (Poland).

Electrophoresis. All samples were evaluated by 1-D gel electrophoresis based on the SDS-PAGE technique was used. PAAG hydrogels (15 %) without Lap and with incorporated Lap, or LapA platelets were placed in the electrophoretic cells between two vertical glass plates (45×75 mm, with spacers 1 mm thick and a comb with eight teeth). The applied voltage was 100 V, and the typical separation time was approximately 3.5 h. For better visualization the samples were stained by Coomassie Brilliant blue G 250 (CI 42655).

Statistical treatment. Data for equilibrium degree of the hydrogels swelling are presented as means and standard errors of the mean values. Statistical comparisons were performed with one-way analysis of variance (ANOVA) for an average of 3–5 replicates. Statistical significance for all tests was set at a P value < 0.05.

RESULTS AND DISCUSSION

Scanning electron microcopy images. General analysis of SEM images revealed the porous structure of the PAAG and PAAG hydrogels with incorporated Lap and LapA platelets. The distributions of interconnected pores with a predominant sizes in the range from 1 to 100 μm were observed. Smaller diameter pores have an elongated, irregular shape and are concentrated in a honeycomb-like (cellular) structure. Larger pores (> 50 μm) have a regular rounded shape with thick walls of about 1–3 μm. Moreover, SEM images at high magnifications revealed large differences for PAAG + Lap (Fig. 2 *a*) and PAAG + LapA (Fig. 2 *b*) samples. Particularly, for PAAG + Lap samples the platelets were deeply integrated in the hydrogel structure. For PPG + LapA samples the formation of fairly shells of aggregated LapA nanoparticles was observed (Fig. 2 *a*). It can be explained by the effects of acid activation on the destruction of crystal lattice of Lap and formation of more active form of LapA with stronger internal bonds [40, 41].

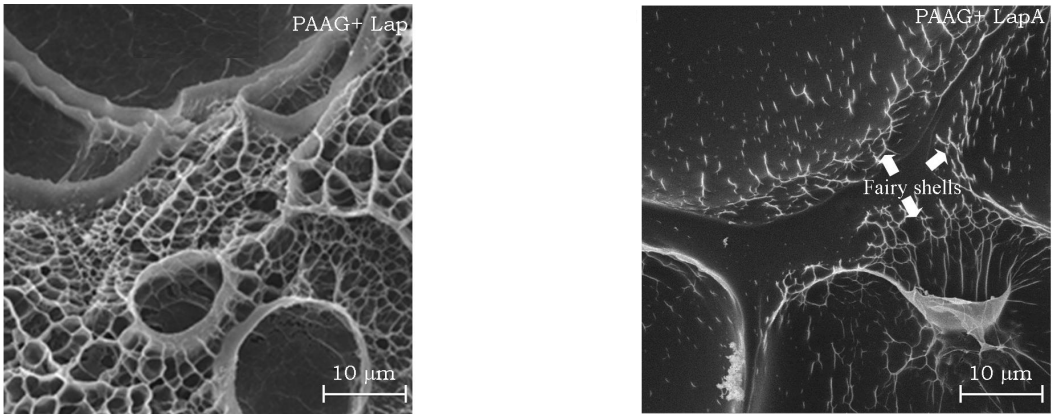

a *b*

Fig. 2. SEM images of PAAG gels with incorporated (0.04 % mass) LAP (*a*) and LapA (*b*). For PAAG + LapA samples (*b*) the formation of fairly shells of aggregated LapA nanoparticles was observed

PAAG + Lap and PAAG + LapA swelling. The swelling degree PAAG based hydrogels was studied in details for optimal concentrations of AA (15 %) and cross-linking agent (0.3 %). In absence of Lap or LapA the maximum swelling degree was about $Q_{max} \approx 8.2$ g/g. Incorporation of Lap or LapA affected the value of Q_{max}. Fig. 3 *a* presents examples of the swelling curves of PAAG samples $Q(t)$ with incorporated LapA platelets at different concentrations of LapA (C_{LapA} = 0–0.16 %). Fig. 3 *b* compares the swelling curves of PAAG samples $Q(t)$ with

incorporated Lap and LapA platelets at the same concentration $C_{Lap} = C_{LapA} = 0.04$ %. Note, that in all cases the maximal equilibrium degree of swelling Q_{max} was reached within the first 5 hours (Fig. 3 *a*, *b*). The concentration of platelets affected the value of Q_{max}, initially it decreased up to the minimum $Q_{max} \approx 7.6$ g/g at $C_{Lap} \approx 0.04$ % and then increased at higher concentrations (inset to Fig. 3 *a*).

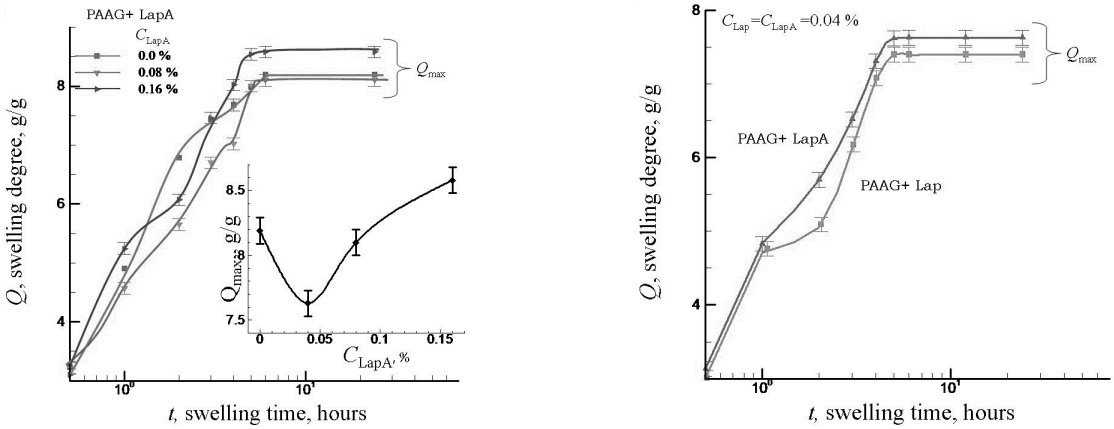

Fig. 3. Equilibrium degree of the hydrogels swelling in distilled water Q versus the swelling time t for PAAG + LapA at different concentration of LapA C_{LapA} (*a*). Here inset shows Q_{max} versus C_{LapA} dependence (*a*), and comparison of $Q(t)$ dependences for PAAG + Lap and PAAG + LapA samples at the same concentrations $C_{Lap} = C_{LapA} = 0.04$ % (*b*). Here Q_{max} is the maximal swelling degree after 24 h

Note that origin of such minimum is still not clear completely. It may reflect the effects activation on structure of LapA and complex changes in interactions between PAAG and Lap/LapA platelets. Impact of sulfuric acid activation on aggregation of LapA platelets in aqueous suspension have been analyzed in detail in our previous work [39]. Particularly for pristine Lap samples, the monomodal distribution of particle size with a maximum at distance $d \approx 4.4$ nm was observed. For relatively small degree of acid activation ($C_a = 0.525$–1.25 % wt.), the average particle size of LapA aggregates increased by about an order of magnitude. Moreover, the bimodal distribution of particle sizes with the intensive maximum at $d \approx 57$ nm and less intensive maximum at $d \approx 205$ nm was observed. With a further increase of acid activation ($C_a = 5$–15 % wt.) the distributions of particles sizes were wide and monomodal with the maxima at $d \approx 149$−235 nm. It reflects the complex impact of acid activation on structure of LapA platelets. During acid activation, the protons penetrate into the Lap layers and attack the structural OH-groups [42]. Moreover, the acid activation may result in many structure transformation of LapA platelets [1, 43]. Typically, the mild acid treatment results in production of protonated products [44, 45], whereas the strong acid treatment, with severe attacks of the oxygen sites results in connection of the octahedral and tetrahedral sheets on the edge of the faces and partial damage of the structure [42, 46]. In general, the acid activation can affect the overall negative charge of LapA faces, specific surface area, and average pore volume [42, 43, 47, 48]. X-ray diffraction data evidenced that under the mild acid activation the LapA platelet crystallinity is mainly retained [49]. Moreover, the increased gallery gap and LapA ordering was observed [50–52]. In contrast, under the more strong acid activation the Lap crystallinity was lost and the transformation into the amorphous products was observed. The same conclusions based on analysis of the FTIR spectra have been made [53]. The hydrogels cross-linked with LapA demonstrated better swelling properties, and higher mechanical strength.

Electrophoretic analysis. Fig. 4 present data of SDS-PAGE 1-D gel electrophoresis analysis of human blood plasma protein fractions obtained from the healthy donors, and colorectal

cancer patients without distant metastases CRC M_0 and with distant metastases CRC M_1. The data are presented for PAAG (*a*), PAAG + Lap (*b*) and PAAG+LapA (*c*) hydrogel samples, and concentration of platelets was the same $C_{Lap} = C_{LapA} = 0.04$ % (*b*, *c*). Preliminary

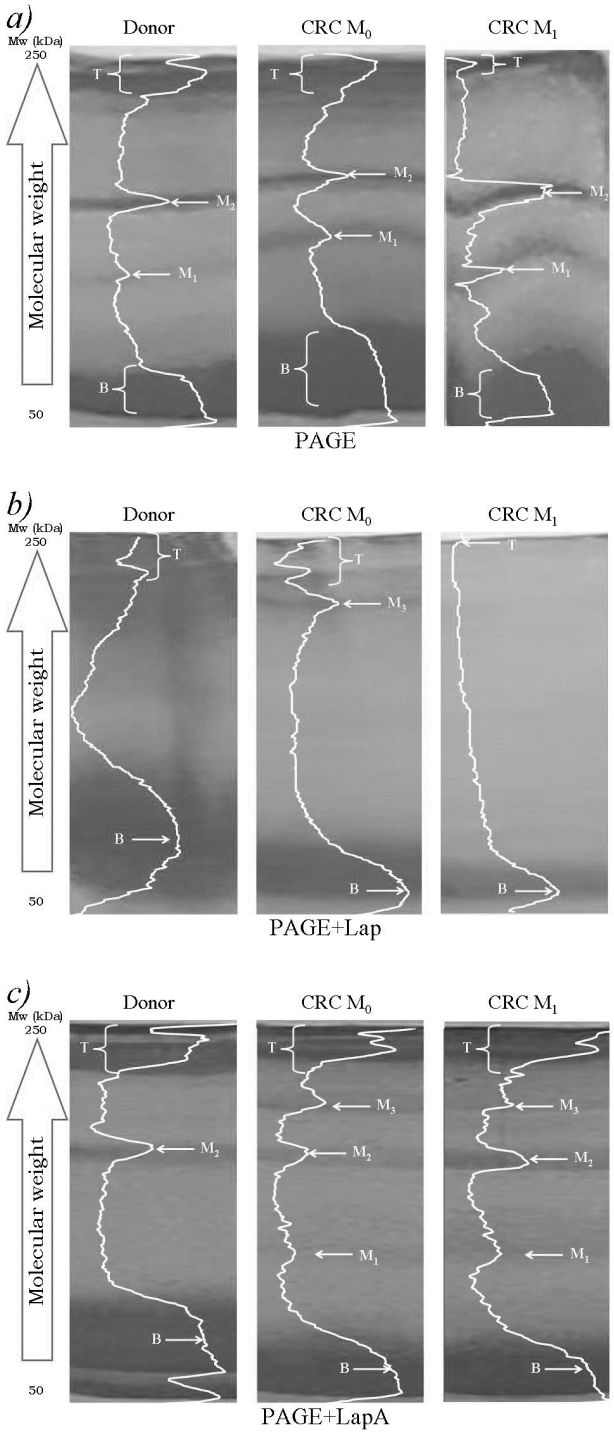

Fig. 4. Electropherograms of human blood plasma protein fractions obtained from the donors, and colorectal cancer patients without distant metastases CRC M_0 and with distant metastases CRC M_1 for PAAG (*a*), PAAG + Lap (*b*), and PAAG + LapA (*c*) hydrogel samples

investigations have elucidated that gels with these concentrations of platelets have the best resolution in relation to blood plasma proteins. Typically the protein spectrum includes different protein bands with a molecular weight distributed with the range ≈ 50–250 kDa [31, 32, 54]. The bottom spots B correspond to the location of the small globular protein (albumin) with the low molecular weights of order 50–70 kDa. The human albumin has a molecular weight of 66.5 kDa. It is the most abundant circulating protein found in plasma. The top spots T correspond the location of low mobility detergent-resistant aggregates. The intermediate spots M_1-M_3 corresponds to the locations of more mobile proteins (*e.g.*, transferrin, fibrinogen, macroglobulin, haptoglobin, ceruloplasmin, lipoprotein *etc.*)

For the PAAG samples 4 protein bands B, M_1, M_2 and T were detected. Some differences between the donor and CRC patient patterns were observed (Fig. 4 *a*). Particularly, the most wide bottom spot B was observed for CRC M_0 patients. For the PAAG + Lap samples all patterns were rather diffused, and only one bottom spot B was observed for CRC M_1 patients (Fig. 4 *b*). The better separation of the fraction of high molecular weight proteins (≈ 100–250 kD) in the PAGE + LapA samples was observed (Fig. 4 *c*). Here, up to 3 bands B, M_2, and T were recorded for donor and up to 5 bands B, M_1, M_2, M_3 and T in patients with CRC. Some differences in the intensity of bands were observed for M_0 and M_1 patients.

Observed positive effects of incorporation of LapA particles into PAAG matrix on protein separation efficiency correlates with the effects of LapA on the swelling degree PAAG based hydrogels (Fig. 4). It may be explained by the effects activation on structure of LapA and complex changes in interactions between PAAG and Lap/LapA platelets.

CONCLUSIONS

Hydrogels with embedded Laponite® platelets and acid activated platelets represent a new generation of materials with promising biomedical application (*e.g.*, diagnostics and therapy). In the current research, the functional hydrogels on base of polyacrylamide hydrogels with incorporated platelets were synthesized and characterized using scanning electron microscopy and swelling techniques. Obtained data evidenced the presence of deep integration of LapA platelets into the hydrogel structure and formation of the shells of aggregated LapA particles. It can be explained by the formation of more active forms of LapA with stronger internal bonds. Effects of LapA concentration on the swelling kinetics and the maximal swelling degree were also evaluated. The electrophoresis technique based on using of polyacrylamide gel with additive of the strong denaturing sodium dodecyl sulfate detergent was applied for analysis of human blood plasma protein fractions for the donors, and colorectal cancer patients without and with distant metastases. The better separation of human plasma proteins was observed in these hydrogels with incorporated acid activated platelets. The testing of developed new materials for diagnostics of different forms of cancer diseases is desirable in future.

ACKNOWLEDGEMENT

The authors are extremely grateful for the financial support of the National Research Foundation of Ukraine (as part of the competition “Science for the Recovery of Ukraine in the War and Post-War Periods”) in the framework of the project “Designing smart biomaterials and functionalized nanoparticles for cancer diagnosis and therapy under stress conditions” (No. 2022.01/0039, 2024).

Синтез та застосування поліакриламідних гідрогелів з інкорпорованим кислотно-активованим Laponite® для діагностики онкологічних захворювань

Ю.М. Самченко, О.А. Самойленко, А.В. Вербиненко, І.І. Ганусевич, Л.О. Керносенко, Т.П. Полторацька, Н.О. Пасмурцева, О.О. Соловйова, І.І. Волобаєв

Інститут біоколоїдної хімії ім. Ф.Д. Овчаренка Національної Академії Наук України
бульв. Академіка Вернадського, 42, Київ, 03142, Україна, yu1sam@yahoo.com
Інститут експериментальної патології, онкології і радіобіології ім. Р.Є. Кавецького Національної Академії Наук України
вул. Васильківська, 45, Київ, 03022, Україна, a-samoilenko@ukr.net

Гідрогелі з інкорпорованими кислотно-активованими пластинками Laponite® (LapA) представляють нове покоління біоматеріалів із перспективним біомедичним застосуванням (наприклад, для діагностики та терапії). Наноматеріали на основі LapA мають високу питому поверхню та демонструють досить привабливі гідрофільні властивості. Фізичне зшивання гідрогелів за допомогою LapA дозволило значно покращити однорідність систем, прозорість і транспорт ліків у цих системах. Загалом включення LapA також може впливати на рівноважний ступінь набухання при фазовому переході від набряклої до зморщеної гідрогелевої фази. У даній роботі досліджено ефективність використання поліакриламідних гідрогелів (PAAG) з інкорпорованим LapA для діагностики онкологічних захворювань. Процедуру синтезу проводили за допомогою ультразвукової обробки водної дисперсії сумішей мономера, зшиваючого агента та ініціаторів. Зразки PAAG+LapA характеризували за допомогою вивчення ступеня набухання та скануючої електронної мікроскопії (SEM). Аналіз SEM зображень свідчить про наявність інтеграції нанопластинок LapA в структуру гідрогелю та формування оболонок агрегованих частинок LapA. Це можна пояснити утворенням більш активних форм LapA з більш міцними внутрішніми зв'язками. Також оцінювали вплив концентрації Lap, LapA на кінетику набухання та максимальний ступінь набухання.Максимальний рівноважний ступінь набухання Q_{max} досягався протягом перших 5 годин. Концентрація нанопластинок впливала на величину Q_{max}, і спочатку вона знижувалася до мінімального значення $Q_{max} \approx 7.6$ г/г при $C_{Lap} = C_{LapA} \approx 0.04$ %, а потім зростала при вищих концентраціях. Для цих зразків спектр поділу білків плазми периферичної крові вивчали за допомогою методу електрофорезу у поліакриламідному гелі з додецилсульфатом натрію (SDS-PAGE). Досліджувалися зразки плазми периферичної крові, отримані від донорів, і пацієнтів з колоректальним раком без віддалених метастазів і з віддаленими метастазами. Краще розділення білків плазми людини спостерігалося в гідрогелях з вбудованими пластинками LapA. У майбутніх дослідженнях бажано перевірити використання цих нових матеріалів для електрофоретичної SDS-PAGE діагностики різних форм онкологічних захворювань.

***Ключові слова**: Пластинки Laponite®, кислотна активація, набухання, SDS-PAGE, діагностика онкологічних захворювань*

REFERENCES

1. Samoylenko O., Korotych O., Manilo M., Samchenko Y., Shlyakhovenko V., Lebovka N. Chapter 15. Biomedical Applications of Laponite-based Nanomaterials and Formulations. In: *Soft Matter Systems for Biomedical Applications*. (Springer Proceedings in Physics, 2022). P. 385.
2. Lebovka N.I., Samchenko Y.M., Kernosenko L.O., Poltoratska T.P., Pasmurtseva N.O., Mamyshev I.E., Gigiberiya V.A. Temperature sensitive hydrogels cross-linked by magnetic LAPONITE® RD®: effects of particle magnetization. *Mater. Adv*. 2020. **1**(8): 2994.
3. Gantenbein D., Schoelkopf J., Matthews G.P., Gane P.A.C. Determining the size distribution-defined aspect ratio of platy particles. *Appl. Clay Sci.* 2011. **53**(4): 544.
4. Balnois E., Durand-Vidal S., Levitz P. Probing the morphology of laponite clay colloids by atomic force microscopy. *Langmuir*. 2003. **19**(17): 6633.
5. Neumann B.S. Behaviour of a synthetic clay in pigment dispersions. *Rheol. Acta.* 1965. **4**(4): 250.
6. Shafran K., Jeans C., Kemp S.J., Murphy K. Dr Barbara S. Neumann: Clay scientist and industrial pioneer; creator of Laponite®. *Clay Miner*. 2020. **55**(3): 1.

7. Tzitzios V., Basina G., Bakandritsos A., Hadjipanayis C.G., Mao H., Niarchos D., Hadjipanayis G.C., Tucek J., Zboril R. Immobilization of magnetic iron oxide nanoparticles on Laponite discs – an easy way to biocompatible ferrofluids and ferrogels. *J. Mater. Chem.* 2010. **20**(26): 5418.
8. Pujala R.K. *Dispersion stability, microstructure and phase transition of anisotropic nanodiscs.* (Switzerland: Springer International Publishing, 2014).
9. Becher T.B., Braga C.B., Bertuzzi D.L., Ramos M.D., Hassan A., Crespilho F.N., Ornelas C. The structure--property relation Laponite® materials: from Wigner glasses to strong self-healing hydrogels formed by non-covalent interactions. *Soft Matter*. 2019. **15**(6): 1278.
10. Gholamipour-Shirazi A., Carvalho M.S., Huila M.F.G., Araki K., Dommersnes P., Fossum J.O. Transition from glass-to gel-like states in clay at a liquid interface. *Sci. Rep.* 2016. **6**: 37239.
11. Morariu S., Teodorescu M. Laponite® – A versatile component in hybrid materials for biomedical applications. *Memoirs of the Scientific Sections of the Romanian Academy*. 2020. **43**: 1.
12. Chimene D., Alge D.L., Gaharwar A.K. Two-dimensional nanomaterials for biomedical applications: emerging trends and future prospects. *Adv. Mater*. 2015. **27**(45): 7261.
13. Tomás H., Alves C.S., Rodrigues J. Laponite®: A key nanoplatform for biomedical applications? *Nanomedicine Nanotechnology, Biol. Med*. 2018. **14**(7): 2407.
14. Das S.S., Neelam, Hussain K., Singh S., Hussain A., Faruk A., Tebyetekerwa M. Laponite-based nanomaterials for biomedical applications: a review. *Curr. Pharm. Des.* 2019. **25**(4): 424.
15. De Melo Barbosa R., Ferreira M.A., Meirelles L.M.A., Zorato N., Raffin F.N. Nanoclays in drug delivery systems. In: *Clay Nanoparticles. Properties and Applications. Micro and Nano Technologie*s. (Elsevier, 2020). P. 185.
16. Ianchis R., Ninciuleanu C.M., Gifu I.C., Alexandrescu E., Nistor C.L., Nitu S., Petcu C. Hydrogel-clay nanocomposites as carriers for controlled release. *Curr. Med. Chem*. 2020. **27**(6): 919.
17. Jayakumar A., Surendranath A., Mohanan P.V. 2D materials for next generation healthcare applications. *Int. J. Pharm.* 2018. **551**(1–2): 309.
18. Mousa M., Evans N.D., Oreffo R.O.C., Dawson J.I. Clay nanoparticles for regenerative medicine and biomaterial design: a review of clay bioactivity. *Biomaterials*. 2018. **159**: 204.
19. Ogunsona E.O., Muthuraj R., Ojogbo E., Valerio O., Mekonnen T.H. Engineered nanomaterials for antimicrobial applications: a review. *Appl. Mater. Today*. 2020. **18**: 100473.
20. Pramanik S., Sundar Das D. Future prospects and commercial viability of two-dimensional nanostructures for biomedical technology. Chapter 9. In: Two-Dimensional Nanostructures for Biomedical Technology. (Elsevier, 2020). P. 281.
21. Zhang J., Zhou C.H., Petit S., Zhang H. Hectorite: Synthesis, modification, assembly and applications. *Appl. Clay Sci*. 2019. **177**: 114.
22. Cai Y., Liu B., Liao M., He L., Zhu C. Application of periareolar mammaplasty with the tissue folding technique in breast reshaping following polyacrylamide hydrogel removal. *Breast Care*. 2020. **15**(2): 157.
23. Choi S.B., Kim J., Kim D., Park J., Lee Y., Park K., Kim E.S., Lee S.M., Kim S.-W. Augmentation Mammoplasty Using Polyacrylamide Hydrogel Injection Can Mimic Breast Cancer After 20 Years: A Case Report. *J. Breast Dis*. 2022. **10**(2): 77.
24. Romero M., Macchione M.A., Mattea F., Strumia M. The role of polymers in analytical medical applications. A review. *Microchem. J.* 2020. **159**: 105366.
25. Xiong C., Chen Y., Xu Y., Jiang W., Yin X., Chen D., Gong X., He T., An Y., Han Y. A review of complications of polyacrylamide hydrogel injection. *Chinese J. Plast. Reconstr. Surg.* 2023. **5**(2): 86.
26. Green M.R., Sambrook J. Polyacrylamide gel electrophoresis. *Cold Spring Harb. Protoc*. 2020. **2020**(12): 525.
27. Sennakesavan G., Mostakhdemin M., Dkhar L.K., Seyfoddin A., Fatihhi S.J. Acrylic acid/acrylamide based hydrogels and its properties-A review. *Polym. Degrad. Stab*. 2020. **180**: 109308.
28. Sepantafar M., Maheronnaghsh R., Mohammadi H., Rajabi-Zeleti S., Annabi N., Aghdami N., Baharvand H. Stem cells and injectable hydrogels: synergistic therapeutics in myocardial repair. *Biotechnol. Adv*. 2016. **34**(4): 362.
29. Magdeldin S. *Gel electrophoresis: Principles and basics*. (BoD--Books on Demand, 2012).
30. Wuethrich A., Quirino J.P. A decade of microchip electrophoresis for clinical diagnostics--a review of 2008–2017. *Anal. Chim. Acta*. 2019. **1045**: 42.
31. Shlyakhovenko V., Samoylenko O. Photopolymerization with EDTA and Riboflavin for Proteins Analysis in Polyacrylamide Gel Electrophoresis. *Protein J.* 2022. **41**(4): 438.
32. Tomascova A., Lehotsky J., Kalenska D., Baranovicova E., Kaplan P., Tatarkova Z. A comparison of albumin removal procedures for proteomic analysis of blood plasma. *Gen. Physiol. Biophys.* 2019. **38**(4): 305.
33. Raykin J., Snider E., Bheri S., Mulvihill J., Ethier C.R. A modified gelatin zymography technique incorporating total protein normalization. *Anal. Biochem*. 2017. **521**: 8.

34. Miller A.J., Roman B., Norstrom E. A method for easily customizable gradient gel electrophoresis. *Anal. Biochem*. 2016. **509**: 12.
35. McCausland J.A., Levine A.D. Colorimetric evaluation of PAGE gradient gels. *Anal. Biochem*. 2020. **594**: 113613.
36. Laemmli U.K. Cleavage of structural proteins during the assembly of the head of bacteriophage T4. *Nature*. 1970. **227**(5259): 680.
37. Brunelle J.L., Green R. One-dimensional SDS-polyacrylamide gel electrophoresis (1D SDS-PAGE). *Methods Enzymol*. 2014. **541**: 151.
38. Anonymous. Laponite. Performance Additives. BYK. Technical Information B-RI 21. 2018.
39. Lebovka N., Goncharuk O., Klepko V., Mykhailyk V., Samchenko Y., Kernosenko L., Pasmurtseva N., Poltoratska T., Siryk O., Solovieva O., Tatochenko M. Cross-Linked Hydrogels Based on PolyNIPAAm and Acid-Activated Laponite RD: Swelling and Tunable Thermosensitivity. *Langmuir.* 2022. **38**(18): 5708.
40. Nakamoto K. *Infrared and Raman spectra of inorganic and coordination compounds, part B: applications in coordination, organometallic, and bioinorganic chemistry*. (John Wiley & Sons, 2009).
41. Badertscher M., Buhlmann P., Pretsch E. *Structure determination of organic compounds. Tables of Spectral Data*. (Springer, 2009).
42. Komadel P. Acid activated clays: Materials in continuous demand. *Appl. Clay Sci*. 2016. **131**: 84.
43. Komadel P., Madejova J. Chapter 7.1 Acid Activation of Clay Minerals. *Developments in Clay Science.* 2006. **1**: 263.
44. Tkáč I., Komadel P., Müller D. Acid-treated montmorillonites – A study by ^{29}Si and ^{27}Al MAS NMR. *Clay Miner.* 1994. **29**(1): 11.
45. Breen C., Madejová J., Komadel P. Characterisation of moderately acid-treated, size-fractionated montmorillonites using IR and MAS NMR spectroscopy and thermal analysis. *J. Mater. Chem.* 1995. **5**(3): 469.
46. Bickmore B.R., Bosbach D., Hochella Jr M.F., Charlet L., Rufe E. In situ atomic force microscopy study of hectorite and nontronite dissolution: Implications for phyllosilicate edge surface structures and dissolution mechanisms. *Am. Mineral.* 2001. **86**(4): 411.
47. Van Rompaey K., Van Ranst E., De Coninck F., Vindevogel N. Dissolution characteristics of hectorite in inorganic acids. *Appl. Clay Sci.* 2002. **21**(5): 241.
48. Franco F., Pozo M., Cecilia J.A., Benitez-Guerrero M., Lorente M. Effectiveness of microwave assisted acid treatment on dioctahedral and trioctahedral smectites. The influence of octahedral composition. *Appl. Clay Sci.* 2016. **120**: 70.
49. Mishra A.K., Kuila T., Kim N.H., Lee J.H. Effect of peptizer on the properties of Nafion--Laponite clay nanocomposite membranes for polymer electrolyte membrane fuel cells. *J. Membr. Sci.* 2012. **389**: 316.
50. Mishra A.K., Chattopadhyay S., Nando G.B. Effect of modifiers on morphology and thermal properties of novel thermoplastic polyurethane-peptized laponite nanocomposite. *J. Appl. Polym. Sci.* 2010. **115**(1): 558.
51. Mishra A.K., Rajamohanan P.R., Nando G.B., Chattopadhyay S. Structure – property of thermoplastic polyurethane – clay nanocomposite based on covalent and dual-modified Laponite. *Adv. Sci. Lett.* 2011. **4**(1): 65.
52. Wheeler P.A., Wang J., Baker J., Mathias L.J. Synthesis and characterization of covalently functionalized laponite clay. *Chem. Mater*. 2005. **17**(11): 3012.
53. Li P., Kim N.H., Hui D., Rhee K.Y., Lee J.H. Improved mechanical and swelling behavior of the composite hydrogels prepared by ionic monomer and acid-activated Laponite. *Appl. Clay Sci.* 2009. **46**(4): 414.
54. Cameron J.M., Bruno C., Parachalil D.R., Baker M.J., Bonnier F., Butler H.J., Byrne H.J. Vibrational spectroscopic analysis and quantification of proteins in human blood plasma and serum. In: *Vibrational Spectroscopy in Protein Research*. (Elsevier, 2020). P. 269.

Received 19.06.2024, accepted 25.11.2024